Generation and Detection of Terahertz Waves Using Low-Temperature-Grown GaAs with an Annealing Process

Kiwon Moon, Jeongyong Choi, Jun-Hwan Shin, Sang-Pil Han, Hyunsung Ko, Namje Kim, Jeong-Woo Park, Young-Jong Yoon, Kwang-Yong Kang, Han-Cheol Ryu, and Kyung Hyun Park

In this letter, we present low-temperature grown GaAs (LTG-GaAs)-based photoconductive antennas for the generation and detection of terahertz (THz) waves. The growth of LTG-GaAs and the annealing temperatures are systematically discussed based on the material characteristics and the properties of THz emission and detection. The optimum annealing temperature depends on the growth temperature, which turns out to be 540°C to 580°C for the initial excess arsenic density of $2\times10^{19}/cm^3$ to $8\times10^{19}/cm^3$.

Keywords: LTG-GaAs, terahertz wave, photomixer.

I. Introduction

A defect-engineered low-temperature grown GaAs (LTG-GaAs) is widely used for the generation and detection of ultra-short terahertz (THz) pulses and continuous-wave THz radiation [1]. The key to this technology is the sub-picosecond carrier lifetime originating from high-density arsenic (As) precipitates in the GaAs layer. The precipitates are generated through the thermal annealing of a non-stoichiometric GaAs layer that is grown by molecular beam epitaxy (MBE) at low temperatures, typically below 300°C [2], [3].

In this work, we investigate the effect of growth temperature and annealing on the material characteristics of LTG-GaAs. The effect of the growth and annealing conditions on the material properties are studied systematically. In addition, we fabricate THz photoconductive antennas (THz PCAs) on the LTG-GaAs surfaces to estimate the effect of the material properties on the THz emission and detection performances. It turns out that the detection efficiency of a PC-antenna strongly depends on the annealing conditions, which are irrelevant to the THz emission characteristics. Our work provides useful information on the optimization of material properties for THz PCAs and the development of advanced THz devices.

II. Engineering of LTG-GaAs Properties

LTG-GaAs on a semi-insulating GaAs (100) wafer is grown using a solid-source MBE system (Compact 61, Riber). The growth rate and temperature of the LTG-GaAs epilayer under a beam equivalent pressure ratio of 20 is 1 μm/hr and between 200°C to 250°C, respectively. Before growing an LTG-GaAs layer, a buffer GaAs layer is grown at 600°C for a desirable crystal quality. The amount of excess As is confirmed by measuring the lattice mismatch between the grown layer and the substrate, as shown in Fig. 1(a). At 200°C, the excess As is about $7.3\times10^{19}/cm^3$ while maintaining the macroscopic crystal quality, which is indicated by undulations in the rocking curves [2], [4]. We select samples grown at 200°C and 230°C for studying the effects of thermal annealing on the material

Manuscript received July 5, 2013; revised Oct. 18, 2013; accepted Oct. 26, 2013.

This work was supported by the Joint Research Projects of ISTK and the Public Welfare & Safety Research Program through the National Research Foundation of Korea (NRF), by the Ministry of Education, Science and Technology-grant #2012-0006565 and also Nano-Material Technology Development Program through the NRF of Korea-grant #2012M3A7B4035095.

Kiwon Moon (phone: + 82 42 860 6326, kwmoon@etri.re.kr), Jeongyong Choi (yongs@etri.re.kr), Jun-Hwan Shin (jhshin7@etri.re.kr), Sang-Pil Han (sphan@etri.re.kr), Hyunsung Ko (hsko85@etri.re.kr), Namje Kim (namjekim@etri.re.kr), Jeong-Woo Park (pjw21@etri.re.kr), Young-Jong Yoon (yyjjong@etri.re.kr), and Kyung Hyun Park (khp@etri.re.kr) are with the Creative Future Research Laboratory, ETRI, Daejeon, Rep. of Korea.

Kwang-Yong Kang (kykang@changwon.ac.kr) is with the Industry-University Cooperation Foundation, Changwon National University, Changwon, Rep. of Korea.

Han-Cheol Ryu (hcryu@syu.ac.kr) is with the Department of Car Mechatronics, Sahmyook University, Seoul, Rep. of Korea.

© 2014 ETRI

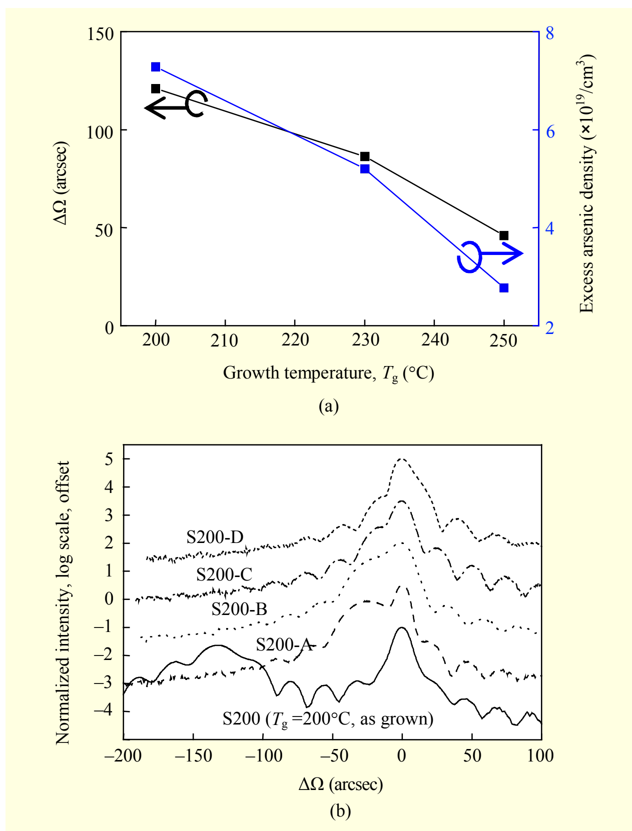

Fig. 1. (a) Excess arsenic density and lattice mismatch as function of growth temperature and (b) effect of annealing temperature on lattice relaxation, as measured by XRD.

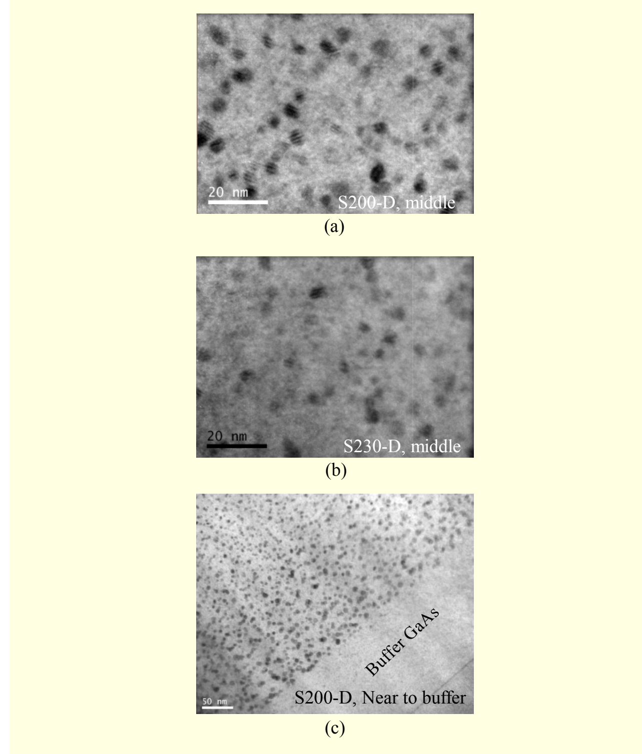

Fig. 2. TEM photographs of annealed LTG-GaAs layers: (a) S200-D, (b) S230-D, and (c) S200-D, which is bottom of layer.

characteristics, such as the carrier lifetime and resistivity. The samples are designated as S200 and S230 for a growth temperature (T_g) of 200°C and 230°C, respectively.

The thermal annealing is performed in a rapid thermal annealing chamber at temperatures ranging from 500°C to 620°C for 10 minutes using a capping GaAs wafer. The annealing temperature (T_a) is denoted by A, B, C, and D for 500°C, 540°C, 580°C, and 620°C, respectively. Thus, as an example, the sample grown at 200°C and annealed at 580°C is noted by S200-C. Owing to the As precipitation in the layer, the lattice mismatch is relaxed after thermal annealing. The lattice mismatch is measured based on XRD rocking curves, as shown in Fig. 1(b). The mismatch is fully relaxed at 620°C.

The As precipitates are observed by transmission electron microscopy (TEM) (Fig. 2). The size of the cluster is a function of T_g and T_a (Fig. 3(a)). The cluster size increases as T_a increases. The cluster size difference between S200 and S230 is insignificant with a T_a of less than 580°C. However, the difference abruptly increases at 620°C (Fig. 3(a)), which implies that most of the antisite is precipitated for S230-D.

Interestingly, for S200-D and S230-D, the cluster diameter increases near the buffer layer (Fig. 2(c)) whereas the diameter

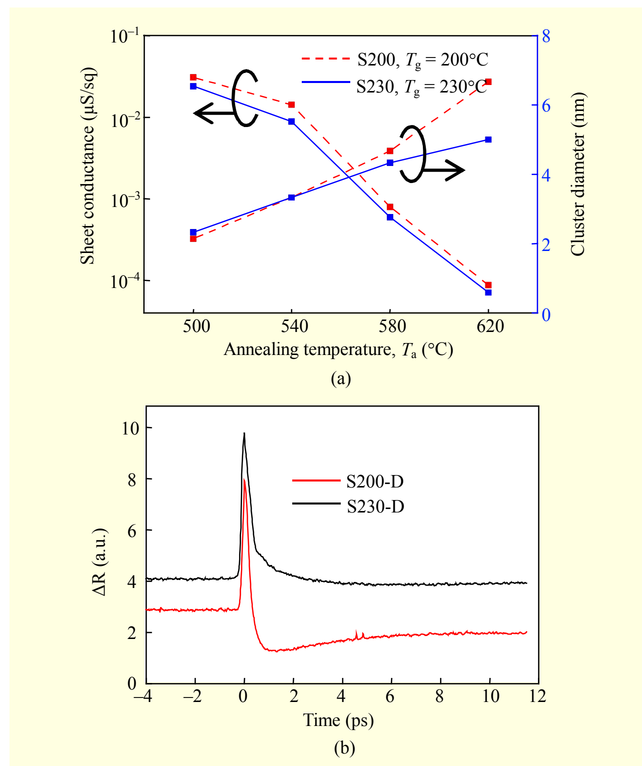

Fig. 3. (a) Sheet conductance and cluster diameter as functions of annealing temperature and (b) transient reflectance for samples annealed at 620°C.

and density of a cluster near to the surface (not shown here) and the middle of the layer are similar. This means that the excess As density is locally increased near the buffer layer, which is attributed to the elongated As diffusion length and the buffer layer that acts as a diffusion barrier. Moreover, the As supply becomes depleted at 620°C, which pushes the precipitation process to the mass-transport limited region. This observation implies that the As clusters can be localized or distributed as designed, opening a door to the achievement of defect-engineered semiconductor devices.

As a result of the precipitation, the As antisite density decreases, suppressing the carrier hopping between the antisites [2]. The As precipitates exhibit metallic properties to generate the depletion region, leading to a high sheet resistance (>10 GΩ/sq) as T_a increases (Fig. 3(a)). This is desirable for photoconductive switching applications, but the carrier lifetime increases as the annealing temperature increases [2], [5]. To circumvent the problem, we confirm the carrier lifetime by the pump-probe transient reflectance measurement.

A Ti:sapphire femtosecond laser pulse with an 860-nm center wavelength is split using a beam splitter for the excitation and the probing, and a mechanical delay line is inserted for a transient measurement. The pulse duration is less than 100 fs, and the optical power for the excitation and probe is 40 mW and 3 mW, respectively. In a previous paper, annealing at 575°C resulted in a carrier lifetime of 0.9 ps [5]. In contrast, the carrier lifetime is suppressed below 0.5 ps even at a T_a of 620°C (Fig. 3(b)) in our experiment. This discrepancy comes from the difference in the initial excess As density. Therefore, the optimum T_a should be determined according to the initial excess As density.

In the transient reflectance curve of S200-D, we observe a negative tail, which is absent in the reflectance of S230-D. Since the negative tail indicates the point defects related to the excess As [2], [4], this also supports the previous observation that the As antisites are depleted in S230-D.

III. THz Generation and Detection Characteristics

We fabricate a simple H-shaped dipole antenna on each of the LTG-GaAs substrates, as shown in the inset of Fig. 4(b). The total size is 2.2 mm × 2.2 mm, including the contact pads. Gaps between the electrodes and the feed point are 20 μm and 6 μm, respectively. The PCAs are used to generate and detect the THz emission, either for the pulse-based time-domain spectroscopy or for the frequency-domain continuous-wave (CW) THz spectroscopy. We use a conventional pulse-based THz time-domain spectroscopy (THz-TDS) setup to estimate the photomixer performances as a generator and detector.

First, we measure reference THz pulses emitted from a photo-excited InAs crystal by the fabricated PCAs. A Ti:sapphire femtosecond laser with a center wavelength of 790 nm is used. The duration is 100 fs, the repetition rate is 80 MHz, and a beam splitter is used to split the laser beam into the pump and the probe for the generation and detection. The pump power and probe power is 300 mW and 12 mW, respectively.

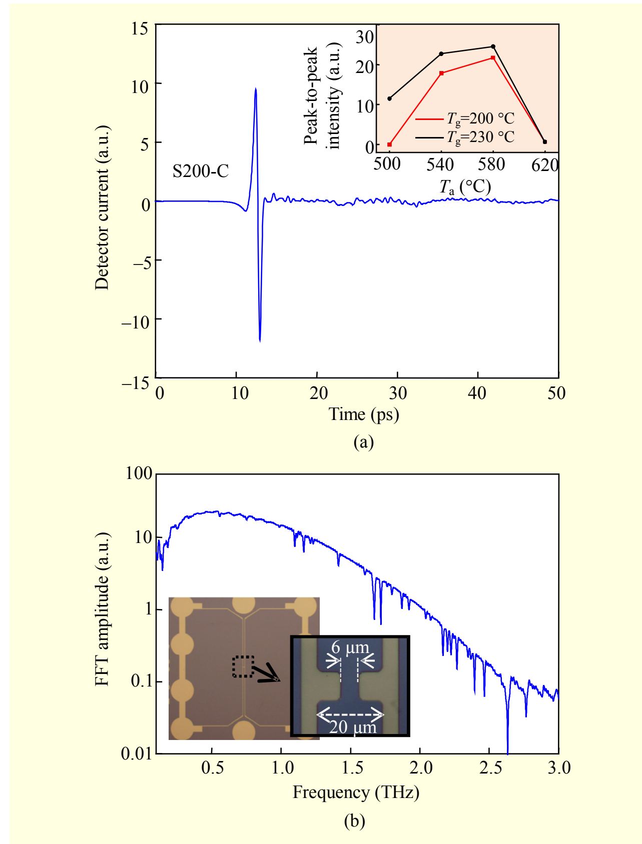

Fig. 4. (a) Time trace of THz pulse emitted from InAs crystal. PCA fabricated on S200-C sample. Inset shows peak-to-peak intensity of detected signal for various substrates. (b) FFT amplitude spectrum of measured THz pulse. Inset is photograph of fabricated THz photomixer.

The detection efficiency is a function of the growth and annealing conditions. The peak-to-peak intensities of the time-domain measurements are shown in the inset of Fig. 4(a). Best performances are observed at annealing temperatures between 540°C and 580°C. However, at 620°C, the detection efficiency significantly degrades. An exemplary time-domain curve is measured by a PCA fabricated on the S200-C sample, which is shown in Fig. 4(a). The amplitude spectrum is presented in Fig. 4(b).

Next, we replace the InAs crystal with the fabricated PCAs to study the THz emission properties. The emitters are biased at 25 V, and the excitation optical power is reduced to 30 mW to prevent the PCAs from experiencing optical damage. A PCA fabricated on S200-C is commonly used for THz detection.

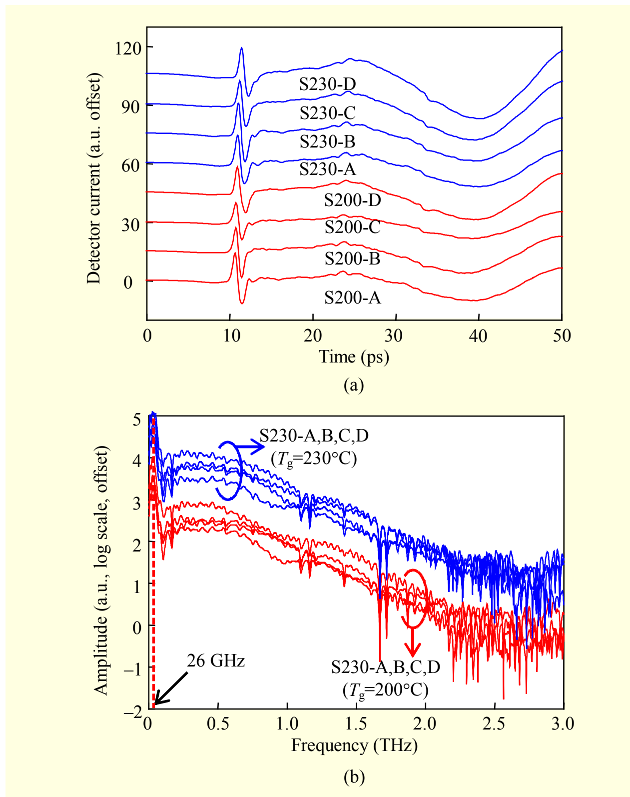

Fig. 5. (a) THz emissions from fabricated PCA. (b) FFT spectra of curves in (a). (Curves are offset for better visibility.)

The emitted THz pulses and their amplitude spectra are shown in Figs. 5(a) and 5(b), respectively. In contrast to the THz detection, the PCAs show similar emission performances in terms of their efficiency and spectral bandwidth, irrespective of T_g and T_a. In general, the spectral bandwidth is known to be affected by the carrier lifetime. In our samples, the carrier lifetimes are all suppressed below 0.5 ps. Therefore, the emission bandwidths are largely unaffected by T_g and T_a.

The differences between the emission and detection characteristics are attributed to the potential barriers at the contact electrodes. To contribute to the conduction between electrodes, the photoelectrons should be accelerated by an external bias to surmount the contact barrier. When used as a THz detector, the bias is provided by the incident THz field, which is extremely weak. Thus, as the substrate becomes highly resistive, only a small fraction of the photoelectrons can surmount the contact barrier, degrading the detection efficiency. However, when used for THz emission, the external bias provides enough energy to surmount the barrier. This roughly explains our results. Note also that after the main peak, low-frequency radiations are observed at 26 GHz (arrow in Fig. 5(b)). The frequency corresponds to the half-wave radiation frequency of the dipole antenna on a GaAs substrate, which is 2.2 mm in total length [6]. Thus, the radiation is thought to be emitted from the contact electrodes and can be suppressed by placing a metallic aperture in the THz beam path or by inserting resistive elements between the feed point and the contact pads [7]. For the CW THz generation, however, the pad radiation is acceptable.

IV. Conclusion

In this work, the growth and annealing conditions for an LTG-GaAs layer were systematically studied. For the THz generation and detection, the annealing temperature should be 540°C to 580°C for excess As density between $2\times10^{19}/cm^3$ to $8\times10^{19}/cm^3$. At the annealing temperature of 620°C, the THz detection efficiency is significantly deteriorated as a result of the increased resistivity. In contrast, the THz emission properties were similar for various growth and annealing conditions. Our work provides systematic information on the material properties for THz emission and detection, and can lead to advanced defect-engineered THz electronic devices.

References

[1] E.R. Brown et al., “Photomixing up to 3.8 THz in Low-Temperature-Grown GaAs,” *Appl. Phys. Lett.*, vol. 66, no. 3, 1995, pp. 285-287.

[2] M.R. Melloch et al., “Low-Temperature Grown III-V Materials,” *Annu. Rev. Mater. Sci.*, vol. 25, no. 25, 1995, pp. 547-600.

[3] M. Tani et al., “Spectroscopic Characterization of Low-Temperature Grown GaAs Epitaxial Films,” *Jpn. J. Appl. Phys.*, vol. 33, 1994, pp. 4807-4811.

[4] X. Liu et al., “Native Point Defects in Low-Temperature-Grown GaAs,” *Appl. Phys. Lett.*, vol. 67, no. 2, 1995, pp. 279-281.

[5] I.S. Gregory et al., “High Resistivity Annealed Low-Temperature GaAs with 100 fs Lifetimes,” *Appl. Phys. Lett.*, vol. 83, no. 20, 2003, pp. 4199-4201.

[6] I.S. Gregory et al., “Resonant Dipole Antennas for Continuous-Wave Terahertz Photomixers,” *Appl. Phys. Lett.* vol. 85, no. 9, 2004, pp. 1622-1624.

[7] B.E. Cole, M.J. Evans, and J. Cluff, *Coherent THz Emitter with DC Power Reducing Resistor*, US Patent 7,397,428 to TeraView Limited, Patent and Trademark Office, Washington, DC, 2008.